Int. J. Solids Structures, 1973, Vol. 9, pp. 363 to 378. Pergamon Press. Printed in Great Britain

ONE-DIMENSIONAL FINITE AMPLITUDE WAVE PROPAGATION IN A COMPRESSIBLE ELASTIC HALF-SPACE

JACOB ABOUDI and YAKO BENVENISTE

School of Engineering, Tel-Aviv University, Ramat-Aviv, Israel

Abstract—The problem of one-dimensional wave propagation of finite amplitude in a nonlinearly elastic compressible half space is considered. The half space is subject on its surface to time dependent arbitrary normal and shear loadings. The problem is solved by employing a certain stable numerical scheme which prevents almost all the numerical oscillations which usually occur near shocks when a standard finite difference scheme is applied.

INTRODUCTION

THE propagation of finite amplitude wave in nonlinearly elastic materials has been investigated by several authors. For a review of the work done in the area and a list of references the reader is referred to a paper by Collins [1] and a recent monograph by Bland [2].

As it can be seen from the literature, most of the work done in the area consists either of general treatments concerning the propagation of finite waves or of analytical solutions which were obtained under rather restrictive conditions on the material constitution and on the applied boundary inputs. On the other hand Fine and Shield [3] formulated perturbation methods in order to handle general elastodynamic problems. This approach was then elaborated by Davison [4] in the study of plane waves and he obtained approximate solutions for the propagation of longitudinal and shear waves in an elastic half-space.

In this paper we deal with one-dimensional finite wave propagation in a nonlinearly elastic half-space. A stable numerical method is given which enables us to deal with completely arbitrary initial and boundary-conditions and general elastic material constitution. The numerical method employs a certain iterative procedure in order to remove the oscillations which are typical in the numerical calculations behind strong gradients such as shock waves which occur in nonlinear problems. Comparing the obtained numerical results with some special cases in which some analytical conclusions could be drawn, it will be shown that the numerical procedure has reliable accuracy. The special cases illustrated are: (1) normal loading, (2) normal loading–unloading, (3) tangential loading, (4) special loading generating a circularly polarized wave. Also to illustrate the fact that the method can handle arbitrary boundary inputs, examples are given with combined normal and tangential loading and loading–unloading. The constitutive equation used for these illustrations is one proposed by Blatz and Ko [5] on the basis of experimental observations as a model for polyurethane foam rubber and has been chosen solely as a matter of convenience.

STATEMENT OF THE PROBLEM

Let us consider a homogeneous isotropic nonlinearly elastic material occupying an infinite half-space $Y \geq 0$. Let the position of the material particles be defined at all times with respect to a fixed cartesian coordinate system (X, Y, Z) where X, Y, Z define the position of the material particles at $t = 0$. For times $t \geq 0$ let us treat a one-dimensional deformation in the form

$$\mathbf{x} = \mathbf{X} + \mathbf{u}(Y, t), \tag{1}$$

where

$$\mathbf{x} = (x, y, z), \qquad \mathbf{X} = (X, Y, Z), \qquad \mathbf{u} = (u, v, w). \tag{2}$$

and x, y, z are the position of the particles in their final configuration. As a stress measure let us use the first Piola–Kirchhoff stress tensor $\mathbf{T}$ [6, p. 222]. $\mathbf{T}$ is related to the Cauchy stress tensor $\boldsymbol{\sigma}$ by the relation [6, p. 222]:

$$\mathbf{T} = J\mathbf{F}^{-1}\boldsymbol{\sigma} \tag{3}$$

where $J = \det \mathbf{F}$ and $\mathbf{F}$ is the deformation gradient tensor with its components F_{iK} defined by:

$$F_{iK} = \frac{\partial x_i}{\partial X_K}. \tag{4}$$

The components of $\mathbf{T}$ are denoted by T_{Ik} and the ones of $\boldsymbol{\sigma}$ by σ_{ik}.

In terms of the first Piola–Kirchhoff stresses, in the absence of body forces the equations of motion are given by [6, p. 224]

$$\begin{aligned} \frac{\partial}{\partial Y} T_{Yx} &= \rho_0 \frac{\partial^2 x}{\partial t^2}, \\ \frac{\partial}{\partial Y} T_{Yy} &= \rho_0 \frac{\partial^2 y}{\partial t^2}, \\ \frac{\partial}{\partial Y} T_{Yz} &= \rho_0 \frac{\partial^2 z}{\partial t^2}, \end{aligned} \tag{5}$$

where ρ_0 is the density of the undeformed body.

In the present work all thermodynamic effects will be ignored. It is known that for a non-heat conducting material, the change in entropy across a shock is of third order in the displacement gradients [2]. Therefore by adopting the adiabatic approximation and treating weak shocks only we can neglect the entropy changes everywhere at all times.

Disregarding all non-mechanical influences, for a general compressible elastic material the Cauchy stresses are given in terms of the displacement gradients by the following relation [7]:

$$\boldsymbol{\sigma} = \chi_0 \mathbf{I} + \chi_1 \mathbf{B} + \chi_{-1} \mathbf{B}^{-1} \tag{6}$$

where

$$\mathbf{B} = \mathbf{F}\mathbf{F}^T \tag{7}$$

and is called the left Cauchy–Green tensor, **I** is the unit matrix, and $\chi_0, \chi_1, \chi_{-1}$ are general functions of the principal invariants of **B**.

Using (6) and (3), the constitutive equation in terms of the first Piola–Kirchhoff stress tensor can be easily obtained. Clearly using equations (1) in the constitutive equations one can express the components of **T** in terms of the displacement gradients $\partial \mathbf{u}/\partial Y$. Using these expressions of T_{Yx}, T_{Yy}, T_{Yz} which are in terms of $\partial \mathbf{u}/\partial Y$, one obtains three coupled non-linear equations of motion for **u**. For stresses prescribed on the surface of the half space we also obtain non-linear expressions for boundary conditions in terms of $\partial \mathbf{u}/\partial Y$ on the boundary.

As a specific constitutive equation we chose in this paper the one proposed by Blatz and Ko [5] as a description of a 47 per cent by volume polyurethane foam rubber having a shear modulus of 32 lb/in^2. According to this constitutive equation the Cauchy stress is given by

$$\boldsymbol{\sigma} = -(\mu/\det F)\mathbf{B}^{-1} + \mu\mathbf{I} \tag{8}$$

where μ is the shear modulus. In case of infinitesimal deformations this equation reduces to the linear stress–strain relation (Hooke's law) with Poisson's ratio $\nu = 1/4$. Using equation (3) we get the expression for the first Piola–Kirchhoff stress

$$\mathbf{T} = -\mu\mathbf{F}^{-1}\mathbf{B}^{-1} + \mu(\det \mathbf{F})\mathbf{F}^{-1}. \tag{9}$$

With the deformation given by (1), the deformation gradient tensor **F** becomes:

$$\mathbf{F} = \begin{bmatrix} 1 & \dfrac{\partial u}{\partial Y} & 0 \\ 0 & 1+\dfrac{\partial v}{\partial Y} & 0 \\ 0 & \dfrac{\partial w}{\partial Y} & 1 \end{bmatrix}, \tag{10}$$

and for the invertibility of the motion (1) we need to satisfy

$$1+\frac{\partial v}{\partial Y} > 0.$$

Using this deformation gradient in (9) we get for T_{Yx}, T_{Yy}, T_{Yz}, the following expressions:

$$\left.\begin{aligned} T_{Yx} &= \mu\left(\frac{\partial u}{\partial Y}\right) \Big/ \left(1+\frac{\partial v}{\partial Y}\right)^2, \\ T_{Yy} &= -\mu\left\{\left[1+\left(\frac{\partial u}{\partial Y}\right)^2+\left(\frac{\partial w}{\partial Y}\right)^2\right] \Big/ \left[1+\frac{\partial v}{\partial Y}\right]^3\right\}+\mu \\ T_{Yz} &= \mu\frac{\partial w}{\partial Y} \Big/ \left(1+\frac{\partial v}{\partial Y}\right)^2. \end{aligned}\right\} \tag{11}$$

Substituting the above expressions into the equations of motion (5) we obtain:

$$\mathbf{A}\frac{\partial^2 \mathbf{u}}{\partial Y^2} = (1/c_0^2)\frac{\partial^2 \mathbf{u}}{\partial t^2} \tag{12}$$

where

$$\mathbf{A} = \begin{bmatrix} 1/3s^2 & -2\dfrac{\partial u}{\partial Y}\Big/3s^3 & 0 \\ -2\dfrac{\partial u}{\partial Y}\Big/3s^3 & \left[1+\left(\dfrac{\partial u}{\partial Y}\right)^2+\left(\dfrac{\partial w}{\partial Y}\right)^2\right]\Big/s^4 & -2\dfrac{\partial w}{\partial Y}\Big/3s^3 \\ 0 & -2\dfrac{\partial w}{\partial Y}\Big/3s^3 & 1/3s^2 \end{bmatrix}, \tag{13}$$

and

$$s = 1+\frac{\partial v}{\partial Y}; \qquad c_0^2 = \frac{3\mu}{\rho_0}.$$

In order that the disturbances propagate through the material as waves, conditions must be met by the elements of the matrix **A** which guarantee that the system (12) be of hyperbolic type. This is insured by the condition that the wave-speeds λ_i of the system be real. Formal computation of these characteristic wave-speeds gives them in the normalized form (with respect to c_0):

$$\begin{aligned} \lambda_1^2 &= \frac{1}{3(1+v_{,Y})^2}, \\ 6\lambda_{2,3}^2 &= \frac{3(1+u_{,Y}^2+w_{,Y}^2)}{(1+v_{,Y})^4}+\frac{1}{(1+v_{,Y})^2} \\ &\quad \pm\left\{\left[\frac{3(1+u_{,Y}^2+w_{,Y}^2)}{(1+v_{,Y})^4}-\frac{1}{(1+v_{,Y})^2}\right]^2+\frac{16(u_{,Y}^2+w_{,Y}^2)}{(1+v_{,Y})^6}\right\}^{\frac{1}{2}} \end{aligned} \tag{14}$$

where

$$\mathbf{u}_{,Y} = \frac{\partial \mathbf{u}}{\partial Y}.$$

It can be easily seen that for these λ_i's to be real we need to have $v_{,Y} > -1$ and

$$\left[\frac{3(1+u_{,Y}^2+w_{,Y}^2)}{(1+v_{,Y})^4}+\frac{1}{(1+v_{,Y})^2}\right] \geq \left\{\left[\frac{3(1+u_{,Y}^2+w_{,Y}^2)}{(1+v_{,Y})^4}-\frac{1}{(1+v_{,Y})^2}\right]^2+\frac{16(u_{,Y}^2+w_{,Y}^2)}{(1+v_{,Y})^6}\right\}^{\frac{1}{2}}$$

which implies

$$u_{,Y}^2+w_{,Y}^2 \leq 3. \tag{15}$$

Note that $v_{,Y} > -1$ is the already obtained condition for the invertibility of the motion. In the special case of the linear problem we obtain

$$\lambda_1^2 = \lambda_3^2 = 1/3 \qquad \lambda_2^2 = 1.$$

For stresses prescribed on the boundary, according to (11) one gets three nonlinear algebraic equations, which must be solved for the displacement gradients in order to obtain the proper boundary conditions for the system (12). This can be easily carried out by the Newton–Raphson or other numerical procedures. Therefore without loss of generality let us assume that the displacement gradients on the boundary are given by

$$\frac{\partial \mathbf{u}(0,t)}{\partial Y} = \mathbf{a}(t) \tag{16}$$

with $\mathbf{a} = (a_1, a_2, a_3)$. Similarly the initial conditions for the problem will be chosen as

$$\frac{\partial \mathbf{u}(Y,0)}{\partial Y} = \boldsymbol{\beta}(Y) \tag{17}$$

with $\boldsymbol{\beta} = (\beta_1, \beta_2, \beta_3)$.

Equations (12), (16), (17) define completely the initial, boundary-value problem which will be solved in the sequel.

NUMERICAL SOLUTION

In the following we propose a finite difference solution to the system (12) with the initial-conditions (17) and boundary-conditions (16). By comparing the numerical results of some special cases in which some analytical conclusions could be drawn it will be shown that the numerical procedure has reliable accuracy.

By replacing the derivatives in (12) by central difference expressions which are correct up to second order in the spatial and temporal increments $\Delta Y, \Delta t$ respectively, the displacements at time $t+\Delta t$ are obtained in terms of their values at t and $t-\Delta t$ as follows:

$$\mathbf{u}(Y, t+\Delta t) = k^2\mathbf{A}[\mathbf{u}(Y+\Delta Y, t)+\mathbf{u}(Y-\Delta Y, t)]+2(\mathbf{I}-k^2\mathbf{A})\mathbf{u}(Y,t)-\mathbf{u}(Y, t-\Delta t) \tag{18}$$

where $k = c_0\Delta t/\Delta Y$.

The matrix $\mathbf{A}$ in (12) contains first order derivatives. These derivatives are now similarly discretized in (18). According to (18) the displacements at the time level $t+\Delta t$ can be calculated whenever the displacements at the previous two-time levels are known.

The three-time level finite difference system (18) is applied at $Y \geq 0$. In order to impose the boundary conditions (16) at $Y = 0$ an auxiliary point is added at $Y = 0-\Delta Y$ extending out of the medium. The values of the displacements at this auxiliary point are calculated by employing the boundary conditions (16) as follows:

$$\mathbf{u}(-\Delta Y, t) = \mathbf{u}(0,t)-\Delta Y\mathbf{a}(t). \tag{19}$$

In order to find a stability criterion of the three-time level non-linear finite difference system we assume local constancy of $\mathbf{A}$ and set according to von Neumann analysis of stability:

$$\mathbf{u}(Y,t) = \mathbf{u}_0\, e^{i\gamma m\Delta Y}\xi^n \tag{20}$$

where $Y = m\,\Delta Y$, $t = n\,\Delta t$, γ are wave numbers and u_0 is a constant vector. Then (18) reduces to:

$$[(-\xi+2-\xi^{-1})\mathbf{I}-4k^2\mathbf{A}\sin^2\varepsilon]\mathbf{u}_0 = 0 \tag{21}$$

with $\varepsilon = \gamma\Delta Y/2$.

In (18) $\mathbf{A}$ is treated as being locally constant such that the analysis of von Neumann affects only the second derivatives in (18). Equation (21) is satisfied if the determinant of its coefficients vanishes. This determinant can be written in the form:

$$|\mathbf{A}-\lambda^2\mathbf{I}| = 0 \tag{22}$$

with

$$\lambda_i^2 = (2-\xi-\xi^{-1})/4k^2 \sin^2 \varepsilon \tag{23}$$

where $\lambda_i^2 (i = 1, 2, 3)$ are the eigenvalues of $\mathbf{A}$ given by (14). Equation (23) can be rewritten in the form:

$$\xi^2 - 2E_i\xi + 1 = 0 \qquad (i = 1, 2, 3) \tag{24}$$

where

$$E_i = 1 - 2k^2\lambda_i^2 \sin^2 \varepsilon.$$

For stability $|\xi| \leq 1$, and this is satisfied if $|E_i| \leq 1$.

Therefore we obtain the following stability conditions:

$$(c_0\Delta t/\Delta Y)^2 \leq 1/\lambda_i^2 \qquad (i = 1, 2, 3). \tag{25}$$

In the special case of linear wave propagation (24) reduces to the well known condition

$$(c_0\Delta t/\Delta Y)^2 \leq 1.$$

Conditions (24) are employed at every time step over all the range $Y \geq 0$ in order to determine the appropriate time increment Δt with which the computations proceed. The finite difference scheme (18) is applied now with $\Delta Y = l/100$ where l is a reference measure of length, and

$$a_1 = a_3 = 0, \qquad a_2(t_1) = [\sin^2(\pi t_1/0{\cdot}8)]H(0{\cdot}8 - t_1), \qquad t_1 = c_0 t/l \tag{26}$$

with $H(t)$ the Heaviside step function. The results for $\partial v/\partial Y$ at $Y/l = 0{\cdot}05, 0{\cdot}1$ are shown as a function of c_0t/l in Fig. 1(a). Severe oscillations exist which begin near the shock front as is shown at the top of the Fig. 1. These oscillations are typical in the numerical calculations behind strong gradients such as shock waves. Thus although the difference scheme is quite satisfactory from the numerical point of view when it is applied to problems possessing a smooth solution, nevertheless when applied to problems which have a discontinuous solution it yields oscillations which are quite strong. These oscillations appear in the neighborhood of discontinuities such as those representing shock waves. A similar situation was encountered when dealing with elastic–plastic wave propagation [9] where such oscillations appeared near the discontinuity in stresses at the elastic–plastic boundary. These oscillations resulting from non-linear instabilities may in time distort the true solution. There are several methods to overcome this phenomenon, such as the artificial viscosity method [8] in which additional terms are added to the difference scheme so that the region of the shock is smeared over several grid points. Thus the surface of discontinuity is replaced by a thin transition layer in which quantities change rapidly but not discontinuously. In [9] an iterative procedure was employed in order to remove these oscillations and to handle the discontinuous stresses. This iterative difference scheme will be employed now in order to remove the resulting oscillations near the discontinuous displacement

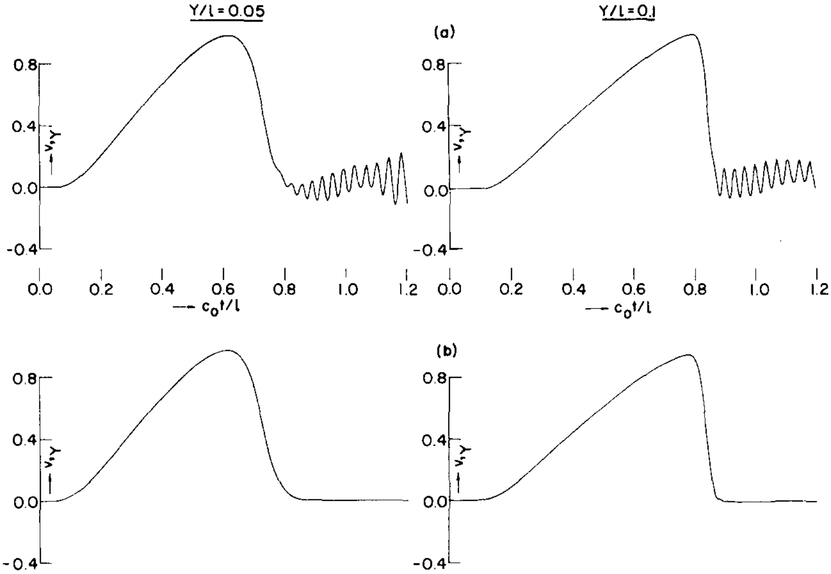

FIG. 1. (a) Normal displacement gradients at stations $Y/l = 0{\cdot}05, 0{\cdot}1$ caused by the prescribed input given by (26) without applying the iterative procedure. (b) Same as (a) with the iterative procedure.

gradients of our problem. Let us define:

$$L[\mathbf{u}(Y,t)] = k^2\mathbf{A}[\mathbf{u}(Y+\Delta Y,t)+\mathbf{u}(Y-\Delta Y,t)-2\mathbf{u}(Y,t)]. \tag{27}$$

Then our previous explicit scheme (18) can be rewritten as follows:

$$\mathbf{u}(Y,t+\Delta t) = 2\mathbf{u}(Y,t)-\mathbf{u}(Y,t-\Delta t)+L[\mathbf{u}(Y,t)]. \tag{28}$$

We consider now instead of (28) the following explicit–implicit difference equation:

$$\mathbf{u}^n(Y,t+\Delta t) = 2\mathbf{u}(Y,t)-\mathbf{u}(Y,t-\Delta t)+\{w_3L[\mathbf{u}^{n-1}(Y,t+\Delta t)] + w_2L[\mathbf{u}(Y,t)] + w_1L[\mathbf{u}(Y,t-\Delta t)]\}/(w_1+w_2+w_3) \tag{29}$$

together with the boundary conditions

$$\mathbf{u}^n(-\Delta Y,t+\Delta t) = \mathbf{u}^n(0,t+\Delta t)-\Delta Y\,.\,\mathbf{a}(t+\Delta t) \tag{30}$$

where n is the number of the iteration $n = 1,2,\ldots,N$, w_i are weight numbers, and $\mathbf{u}^0(Y,t+\Delta t)$ is defined to be equal to the displacement vector $\mathbf{u}(Y,t+\Delta t)$ given by equation (28) which results from the previous difference scheme. Actually (28–30) can be regarded as a predictor-corrector where (29–30) serves as the corrector which is applied N times each of which uses results of the former step. This type of difference scheme is called by Abarbanel and Goldberg [10] an "external" iterative scheme. In [10] computational comparisons for the problem of one-dimensional time dependent cylindrical shock wave in a compressible gas are given between the "external" and the so-called "internal" schemes, where the latter was employed previously by Abarbanel and Zwas [11]. Actual computations which employ the iterative method (28–30) show as in [9] that one iteration only ($N = 1$) removes all the oscillations near the shock and that applying two iterations ($N = 2$) yields results which are as good as the results furnished by one iteration only. Indeed the results from two iterations were indistinguishable from those obtained from one iteration only. In the sequel all results are given with $N = 1$.

Let us carry out the stability analysis of the iteration procedure (28–29). With one iteration ($N = 1$) we obtain:

$$\mathbf{u}^1(Y, t+\Delta t) = \{2+(\theta_2+2\theta_3)L+\theta_3 L^2\}[\mathbf{u}(Y,t)]+\{(\theta_1-\theta_3)L-1\}[\mathbf{u}(Y,t-\Delta t)] \quad (31)$$

where

$$\theta_i = w_i/(w_1+w_2+w_3), \qquad (i = 1, 2, 3).$$

Applying again (20) for $\mathbf{u}^1$ we obtain instead of (21) the following system of equations:

$$\{(-\xi+2)\mathbf{I}-4(\theta_2+2\theta_3)k^2\mathbf{A}\sin^2\varepsilon+16\theta_3 k^4\mathbf{A}^2\sin^4\varepsilon-[\mathbf{I}+4(\theta_1-\theta_3)k^2\mathbf{A}\sin^2\varepsilon]\}\mathbf{u}_0 = 0. \quad (32)$$

Equation (32) is satisfied if the determinant of its coefficients vanishes:

$$|\bar{\mathbf{A}}-\bar{\lambda}_i\mathbf{I}| = 0 \quad (33)$$

where

$$\bar{\mathbf{A}} = 16\theta_3\xi k^4\mathbf{A}^2\sin^2\varepsilon+4k^2\sin^2\varepsilon[\theta_3-\theta_1-(\theta_2+2\theta_3)]\mathbf{A} \quad (34)$$

and $\bar{\lambda}_i^2$ ($i = 1, 2, 3$) are the eigenvalues of the matrix $\bar{\mathbf{A}}$. According to the Cayley–Hamilton theorem, the eigenvalues $\bar{\lambda}_i^2$ are given in terms of λ_i^2 by the same combination by which $\bar{\mathbf{A}}$ is expressed in terms of $\mathbf{A}$ in (34). Hence $\bar{\lambda}_i^2$ are determined in terms of the known quantities λ_i^2 given by (14). Accordingly we obtain similar to (24) the following conditions

$$\xi^2-2\bar{E}_i\xi+\bar{F}_i = 0 \quad (35)$$

where

$$\left.\begin{aligned}\bar{E}_i &= 1+8\theta_3\lambda_i^4k^4\sin^4\varepsilon-2(\theta_2+2\theta_3)\lambda_i^2k^2\sin^2\varepsilon\\ \bar{F}_i &= 1-4(\theta_3-\theta_1)\lambda_i^2k^2\sin^2\varepsilon.\end{aligned}\right\} \quad (36)$$

For stability $|\xi| \le 1$, hence $|\bar{E}_i| \le 1$ and $|\bar{F}_i| \le 1$. These two conditions can be satisfied if:

$$\left.\begin{aligned}&\theta_3 \ge \theta_1, \qquad \theta_3 \ge 0\\ &(c_0\Delta t/\Delta Y)^2 \le 0{\cdot}5/(\theta_3-\theta_1)\lambda_i^2\\ &(c_0\Delta t/\Delta Y)^2 \le (2\theta_3+\theta_2)/4\theta_3\lambda_i^2.\end{aligned}\right\} \quad (37)$$

Note that by their definition and the inequality $\theta_3 \ge \theta_1, 2\theta_3+\theta_2 > 0$. We choose the following weight factors which yield the best results: $w_1 = -1, w_2 = w_3 = 1$. Hence according to (37) the present stability conditions reduce to one half the previous conditions (25) of the noniterative scheme as was similarly obtained in [9].

In Fig. 1(b) the results for the normal displacement gradients with the same boundary conditions (26), obtained this time by applying the iterative procedure (with one iteration) are shown. It is seen that the iteration is very effective in removing the oscillations and does not have the disadvantage of serious smearing of the displacement gradients discontinuity. The features of this method of solution will be checked and discussed in the next section.

RESULTS

Let us compare our numerical results with some analytical conclusions known for some specific loadings. All the results were carried out with $\Delta Y = l/100$.

(a) *Normal loading only*

The boundary conditions in this case are given by (16) with

$$\left.\begin{aligned} a_1(t) &= a_3(t) = 0 \\ a_2(t) &= f(t) \end{aligned}\right\} \tag{38}$$

where

$$f(t) = \delta_2[t^2 H(t)/2] \tag{39}$$

δ_2 is a second order finite difference operator given by

$$\delta_2[q(t)] = [q(t) - 2q(t-\tau) + q(t-2\tau)]/\tau^2 \tag{40}$$

where τ is a time constant.

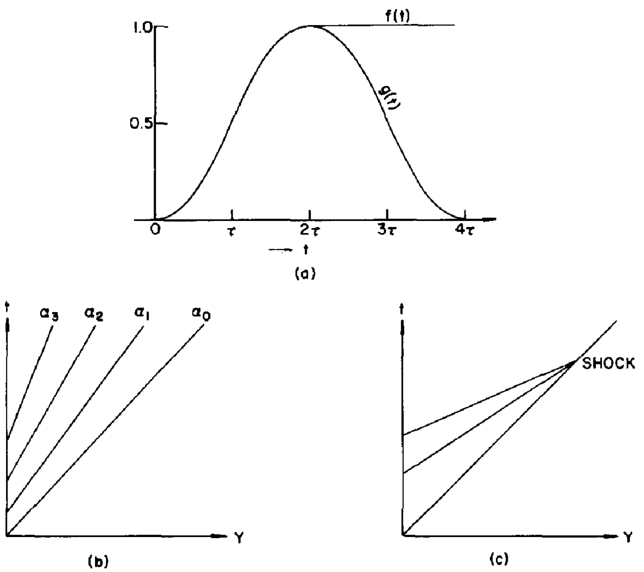

FIG. 2. (a) The time inputs $f(t)$, $g(t)$ given by (39) and (52) respectively. (b) Simple wave with spreading characteristics. (c) Converging characteristics and formation of the shock.

The function $f(t)$ rises from zero at $t = 0$, up to 1·0 at $t = 2\tau$ see Fig. 2(a). The initial conditions (17) will be taken as $\boldsymbol{\beta} = \mathbf{0}$. In the present case the differential equation governing the motion is given by

$$c_0^2 \frac{\partial^2 v}{\partial Y^2} \bigg/ (1+s)^4 = \frac{\partial^2 v}{\partial t^2}. \tag{41}$$

The analytical solution of the above equation in the absence of shocks is given by [12]:

$$\frac{\partial v}{\partial Y}(Y, t) = f\left[t - \left(Y/c\left(\frac{\partial v}{\partial Y}\right)\right)\right] \tag{42}$$

where

$$c\left(\frac{\partial v}{\partial Y}\right) = c_0/(1+s)^2. \tag{43}$$

It is known that [12] according to the form of the function $f(t)$, the solution is either a simple wave with spreading straight characteristics or with converging straight characteristics at the intersection of which a shock forms. The solution (42) is valid for all $Y \geq 0$ and $\alpha = t - Y/c \geq 0$ in the first case, and only up to shocks in the second case. If we call the straight characteristics issuing from $Y = 0$ in Fig. 2(b), the α characteristics, then the condition for no shocks can be written as [12]:

$$\frac{\partial c}{\partial \alpha} < 0. \tag{44}$$

In other words, this is the condition for the spreading out of the characteristics. For our material, according to (43)

$$\begin{aligned} c &= c_0/(1+f(\alpha))^2 \\ \frac{\partial c}{\partial \alpha} &= -[2c_0 f'(\alpha)]/[1+f(\alpha)]^3 \end{aligned} \tag{45}$$

Therefore for $f'(\alpha) > 0$ the characteristics will spread out and for $f'(\alpha) < 0$ they will converge. More explicitly, for positive normal loading no shock will form and for negative normal loading a shock will form (Fig. 2c). In order to use the analytical solution for $t \geq 0, \alpha \geq 0$ we subject the half space to the monotonically non-decreasing function $f(t)$ given in equation (39). The numerical and analytical results are compared in Fig. 3(a) together with the solution of the linear case. The rise time chosen is $2\tau c_0/l = 0{\cdot}4$. Note that the nonlinear effect exhibits itself as a spreading of the pulse over a longer time interval. The maximum deviation of the numerical results from the analytical solution over the whole interval is found to be about 3 per cent. In the linear case the pulse propagates with no change in shape. The convergence of the numerical results to the expected constant value serves also as a check for the accuracy of the numerical procedure.

(b) *Normal loading-unloading*

Now we subject the surface of the half space to a monotonically increasing and then decreasing normal input $h(\alpha)$ in order to observe the formation of a shock. The point in the Y, t plane at which the shock forms initially can be determined analytically and this location can be compared with the one obtained from the numerical procedure.

In order to find this location we observe that the straight α characteristics form a family of lines in the Y, t plane with the parameter α. We are interested in finding the envelope of this family and its cusp at which the shock forms [13]. The equation of an α characteristic is given by (44) with $c = c(\alpha)$. The envelope of this family of lines is parametrically given by

$$\begin{aligned} t &= \alpha + \left[c(\alpha) \Big/ \frac{\partial c}{\partial \alpha}\right] \\ Y &= [c(\alpha)]^2 \Big/ \frac{\partial c}{\partial \alpha}. \end{aligned} \tag{46}$$

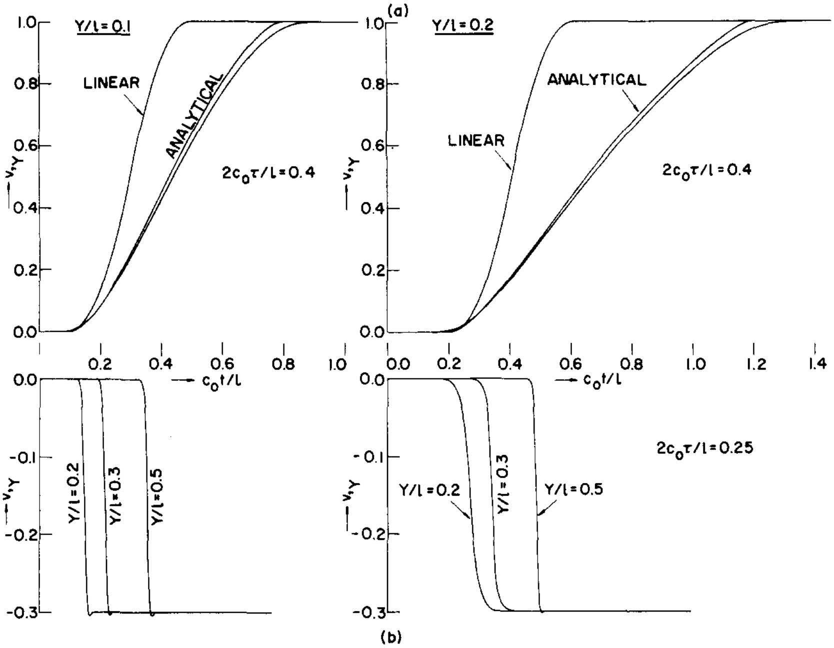

FIG. 3. (a) Analytical and numerical solutions for the normal displacement gradient at stations $Y/l = 0{\cdot}1$, $0{\cdot}2$ caused by $f(t)$. The corresponding linear solution is also shown. (b) Normal displacement gradients caused by $-0{\cdot}3H(t)$ and $-0{\cdot}3f(t)$ respectively.

The cusp is located at the value of α which makes t a minimum i.e.

$$\frac{\partial t}{\partial \alpha} = 0$$

and α is obtained from

$$2\left[\frac{\partial c}{\partial \alpha}\right]^2 = c(\alpha)\frac{\partial^2 c}{\partial \alpha^2}. \tag{47}$$

Using

$$c = c_0/[1+h(\alpha)]^2,$$

we obtain

$$2\left[\left(\frac{\partial h}{\partial \alpha}\right)^2 + \frac{\partial^2 h}{\partial \alpha^2}(1+h)\right] \bigg/ (1+h)^6 = 0,$$

which gives

$$\left(\frac{\partial h}{\partial \alpha}\right)^2 + \frac{\partial^2 h}{\partial \alpha^2}(1+h) = 0. \tag{48}$$

Knowing the function h we can determine on which characteristic the cusp is located, i.e. where the shock forms. As an example let us choose the input function given by:

$$h(\alpha) = \sin^2(\pi\alpha_1/0{\cdot}8)H(0{\cdot}8-t_1), \qquad \alpha_1 = c_0\alpha/l.$$

Substituting in (48) we get for α: $c_0\alpha/l = 0{\cdot}255 \sin^{-1}(0{\cdot}8) = 0{\cdot}565$. Hence according to (46) we obtain

$$Y/l = 0{\cdot}081$$

$$c_0 t/l = 0{\cdot}782.$$

Indeed it can be seen from the numerical results in Fig. 1(b) that at $Y/l = 0{\cdot}05$ the shock has not formed yet, whereas at $Y/l = 0{\cdot}1$ the presence of the shock is observed.

Its arrival time at $Y/l = 0{\cdot}1$ is $c_0 t/l = 0{\cdot}83$. Thus the numerical results are in accordance with the values obtained above analytically. In this case we note the spreading of the pulse until the peak due to loading, and its narrowing after the peak due to unloading. The displacement gradient converges to the constant final value zero as expected.

(c) *Normal negative loading*

As a third example with normal loading only, we choose

$$h(t) = -0{\cdot}3\, H(t).$$

It is known from [2] that this disturbance propagates as a shock with a velocity

$$V = [(\mu/\rho_0 p)(1 - 1/(1+p)^3]^{\frac{1}{2}}. \tag{49}$$

Where p is the jump in $\partial v/\partial Y$ across the shock. The shock is expected to propagate without a change in its strength with the above velocity. For our specific input of $p = -0{\cdot}3$ we get $V = 1{\cdot}46c_0$. The numerical method furnishes quite exactly these analytical results (see Fig. 3(a)). Indeed it gives $0{\cdot}3$ as the correct magnitude of the jump across the shock and confirms that the strength of the shock remains constant as it propagates yielding the value $1{\cdot}47c_0$ for the propagation velocity.

As another example of normal loading only, we subject the surface to a continuously rising negative loading $h(t) = -0{\cdot}3\, f(t)$ with $2\tau c_0/l = 0{\cdot}25$ instead of a step input. Here, contrary to the positive loading case the characteristics converge instead of spreading out and a shock is formed. This fact is again clearly seen in the numerical results (Fig. 3(b)). In this figure we show the disturbance at two observation points $Y/l = 0{\cdot}2, 0{\cdot}3$ before the shock formation and at $Y/l = 0{\cdot}5$ with the presence of the shock. Again the convergence of the numerical results to the expected constant final values is observed.

(d) *Shear loading*

Here we subject the surface of the half-space to the following boundary conditions

$$a_1(t) = H(t), \qquad a_2 = a_3 = 0,$$

and zero initial conditions. In [14] it has been proved that a centered simple wave in $\partial u/\partial Y$ and a shock in $\partial v/\partial Y$ is obtained. The velocity of the shock is again given by (49) where p is the jump across the shock and is negative in this specific case [14]. The solution in the Y, t plane is represented in Fig. 4(a). The numerical solution at stations $Y/l = 0{\cdot}1, 0{\cdot}2, 0{\cdot}3$ is shown in Fig. 4(b) with the value of the jump $p = 0{\cdot}23$. According to (49) we get for the velocity of the shock $V = 1{\cdot}31c_0$.

Note that we get the same shock strength at different stations as predicted in [14]. The shear disturbance is smoothened out as expected and the displacement gradients converge to their expected final values. In this case we note the occurrance of the longitudinal

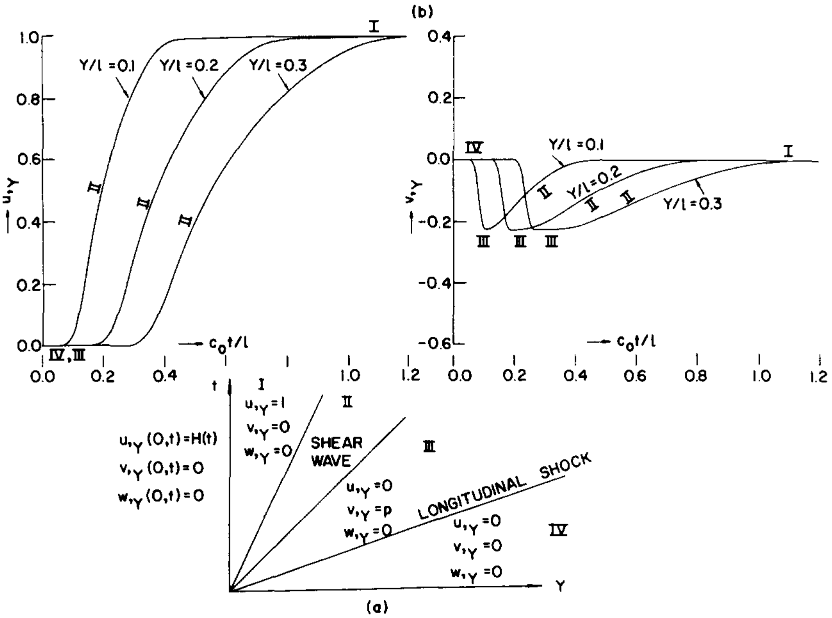

FIG. 4. (a) Characteristics in the Y, t plane for the shear step loading case. (b) Tangential and normal displacement gradients caused by shear step loading.

disturbance which does not occur in the corresponding problem of the linear theory. This disturbance is of smaller order as compared with the corresponding tangential displacement gradient. On the curves of Fig. 4(b), the regions of Fig. 4(a) are indicated for a better depiction of the solution. Note that the width of region II increases as the distance Y increases, a fact which is easily observed in Fig. 4(a).

(e) *Circularly polarized wave*

Bland [2] has shown that there are six simple waves that propagate in a given direction in a nonlinear compressible elastic solid, three in each sense. For an isotropic material, one of these three is circularly polarized, the other two plane polarized. To conclude our checks we produce the circularly polarized wave by applying the proper inputs on the surface of the half space.

Proceeding in the same way as in [2] for our specific material we find that the circularly polarized wave propagates with a velocity given by

$$c_1 = (\mu/\rho_0)^{\frac{1}{2}}/(1+s)^2. \tag{50}$$

Besides, in the simple wave the following equalities are satisfied.

$$\frac{\partial v}{\partial Y} = k_1, \qquad \left(\frac{\partial u}{\partial Y}\right)^2 + \left(\frac{\partial w}{\partial Y}\right)^2 = k_2. \tag{51}$$

Where k_1 and k_2 are constants. Hence the velocity (50) is constant and all the characteristics have the same slope. The value of the constants are determined from the boundary characteristic, i.e. from the initial values in our case. Then the boundary inputs also must satisfy the conditions in (51). Specifically we choose the initial conditions $\beta_1 = \beta_2 = 0, \beta_3(Y) = 1$, and the boundary conditions

$$a_1(t) = 0{\cdot}8\, f(t), \qquad a_2(t) = 0$$
$$a_3(t) = [1-a_1^2(t)]^{\frac{1}{2}}$$

with $2c_0\tau/l = 0{\cdot}4$.

With the above values the velocity (50) becomes $c_1 = (\mu/\rho_0)^{\frac{1}{2}}$. Thus in the solution we expect $\partial v/\partial Y$ to remain zero and the disturbances in $\partial u/\partial Y$ and $\partial w/\partial Y$ to propagate with the above velocity and with no change in shape in such a way that the sum of their squares is equal to one. These results are completely achieved by the obtained numerical solution as shown in Fig. 5. In this figure the normal displacement gradient is not shown since it is effectively zero as expected.

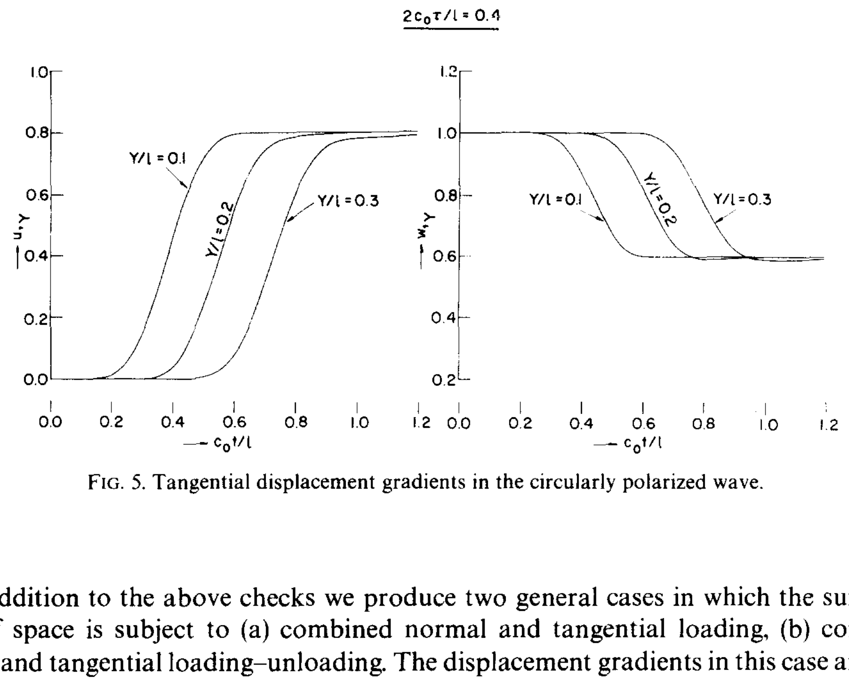

FIG. 5. Tangential displacement gradients in the circularly polarized wave.

In addition to the above checks we produce two general cases in which the surface of the half space is subject to (a) combined normal and tangential loading, (b) combined normal and tangential loading–unloading. The displacement gradients in this case are given in Figs. 6 and 7. In Fig. 6 we choose $2c_0\tau/l = 0{\cdot}2, 0{\cdot}15, 0{\cdot}1$ as the rise times of the applied inputs $f(t)$ defined by (39) in the X, Y, and Z directions respectively. In Fig. 7 we choose the loading–unloading function $g(t)$ defined by:

$$g(t) = \delta_2[t^2H(t)/2] - \delta_2[(t-2\tau)^2H(t-2\tau)/2] \tag{52}$$

The function $g(t)$ rises from 0 at $t = 0$ up to 1·0 at $t = 2\tau$ and then drops back to 0 at $t = 4\tau$ (see Fig. 2(a)).

We choose the time durations $4c_0\tau/l = 0{\cdot}2, 0{\cdot}15, 0{\cdot}1$ in the X, Y, and Z directions respectively. Here again the displacement gradients converge to the expected final constant values after the proper time has elapsed.

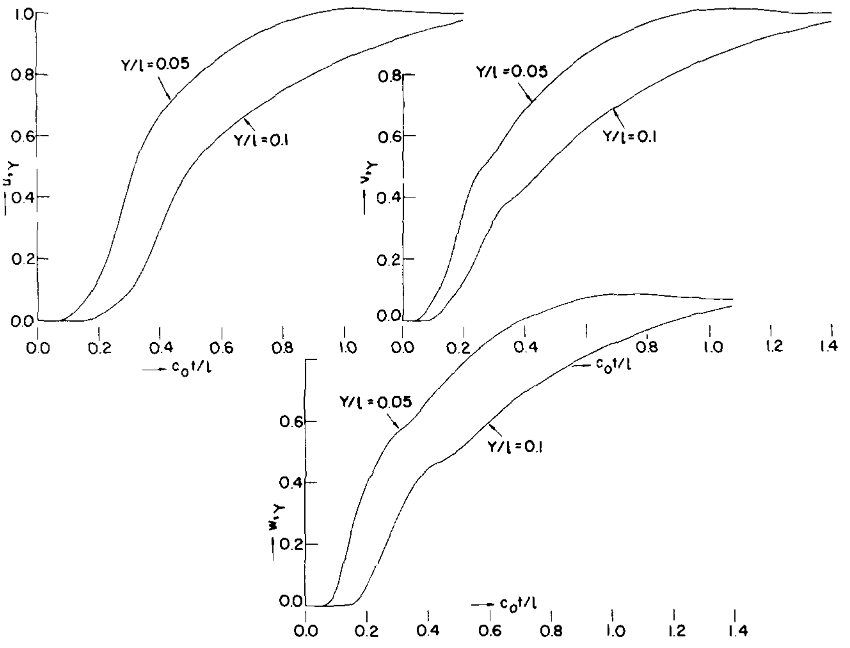

FIG. 6. Normal and tangential displacement gradients caused by combined normal and tangential loadings.

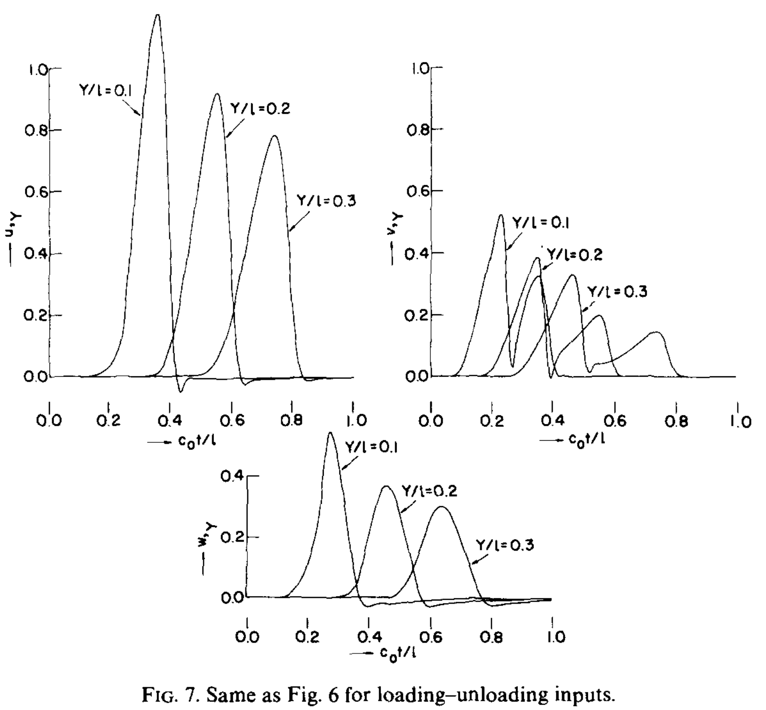

FIG. 7. Same as Fig. 6 for loading–unloading inputs.

REFERENCES

[1] W. D. COLLINS, One-dimensional nonlinear wave propagation in incompressible elastic materials. *Q. Jl Mech. Appl. Math.* **19**, 259–328 (1966).
[2] D. R. BLAND, *Nonlinear Dynamic Elasticity*. Blaisdell (1969).
[3] A. D. FINE and R. T. SHIELD, Second order effects in the propagation of elastic waves. *Int. J. Solids Struct.* **2**, 605–620 (1966).
[4] L. DAVISON, Peturbation theory of nonlinear elastic wave propagation. *Int. J. Solids Struct.* **4**, 301–322 (1968).
[5] P. BLATZ and W. L. KO, Application of finite elasticity theory to the deformation of rubbers. *Trans. Soc. Rheology* **6**, 223–251 (1962).
[6] E. L. MALVERN, *Introduction to the Mechanics of a Continuous Medium*. Prentice-Hall (1969).
[7] C. TRUESDELL and W. NOLL, The nonlinear field theories of mechanics, *Handbuch der Physik* III/III, edited by S. FLUGGE. Springer (1960).
[8] R. D. RICHTMYER and K. W. MORTON, *Difference Methods for Initial-Value Problems*, 2nd edition. Interscience (1967).
[9] J. ABOUDI, Wave propagation from a spherical cavity imbedded in an elasto-plastic medium. *J. Engng Math.* **5**, 279–287 (1971).
[10] S. ABARBANEL and M. GOLDBERG, Numerical solution of quasi-conservative hyperbolic systems—the cylindrical shock problem. *J. Comp. Phys.* To be published.
[11] S. ABARBANEL and G. ZWAS, An iterative finite difference method for hyperbolic systems. *Math. Comp.* **23**, 549–565 (1969).
[12] A. JEFFREY and T. TANIUTI, *Nonlinear Wave Propagation*. Academic Press (1964).
[13] W. D. COLLINS, The propagation and interaction of one-dimensional nonlinear waves in an incompressible isotropic elastic half-space, *Q. Jl Mech. Appl. Math.* **20**, 429–452 (1967).
[14] L. DAVISON, Propagation of plane waves of finite amplitude in elastic solids, *J. Mech. Phys. Solids* **14**, 249–270 (1966).

Acknowledgement—The computations reported in this paper were carried out on the CDC-6600 Computer at the Tel-Aviv University Computation Center.

(*Received* 4 *February* 1972; *revised* 26 *July* 1972)

Абстракт—Исследуется задача распространения одномерной волны конечной амплитуды в нелинейно упругом сжимаемом полупространстве. Полупространство подвержено на его поверхности действию зависящем от времени, произвольных нагрузок нормальной и сдвига. Задача решается путем применения некоторой устоичивой численной схемы которая предотвращает почти всем численным колебаниям, которые обычно порисходят близи ударов, для случая стандартной схемы в конечных разностях.